IOP Conf. Series: Journal of Physics: Conf. Series **1063** (2018) 012048 doi:10.1088/1742-6596/1063/1/012048

Crystal plasticity analysis of the deformation of a grade 2 CP-Ti oligocrystal

Pierre Baudoin[1], Takayuki Hama[1], Sohei Uchida[2], Hirohiko Takuda[1]

[1] Graduate School of Energy Science, Kyoto University, Yoshida-Honmachi, Sakyo-ku, Kyoto 606-8501, Japan

[2] Osaka Research Institute of Industrial Science and Technology, 2-7-1, Ayumino, Izumi-city, Osaka 594-1157, Japan

E-mail: pierre.baudoin@centraliens-lille.org

Abstract. In recent years, direct comparisons between simulations and experiments dedicated to test samples containing a small number of grains (oligocrystals) instrumented using full field measurements techniques (DIC, grid method) have proved fruitful to investigate and accurately reproduce the behavior of BCC and FCC crystals. The extension of this approach to HCP metals and CP-Ti in particular is the objective of the present work. The deformation behavior of a grade 2 CP-Ti material is investigated numerically, by comparing the predictions of strain field in a 32 grains oligocrystal loaded in tension with experimental results. It is found that the set of constitutive parameters identified by the authors in a previous study [Hama et al., Int. J. Plast., 2017(91), 77] reflects the experimental behavior satisfactorily for strain fields.

1. Introduction

Hexagonal-close-packed (HCP) alloys such as magnesium and titanium exhibit strong deformation anisotropy, owing to the low degree of symmetry of the crystal lattice and the occurrence of twinning and de-twinning. Crystal plasticity analysis is an essential tool to accurately reproduce this behavior numerically [1]. Many specificities of the behavior, such as tension-compression asymmetry, texture evolution and stress-strain curves can thus be reproduced. However, the precise identification of the numerous constitutive parameters of the numerical model remains challenging. In particular, and contrary to body-centered cubic (BCC) and face-centered cubic (FCC) metals, critical resolved shear stresses (CRSSs) vary according to the considered slip system family. In the case of commercially-pure titanium (CP-Ti), the exact ratios between CRSSs of different families are still being discussed [2, 3, 4]. This point is mainly due to the difficult identification of precise CRSS values from comparison with typical experiments, i.e., stress-strain curves and texture evolution.

In recent years, an approach based on the systematic comparison between full-field measurements (displacement, strain, temperature in some cases) and crystal plasticity simulations of oligocrystals, i.e. samples containing up to a few dozen grains, has shown promise to refine the identification of the constitutive parameters for crystal plasticity analysis [5, 6, 7]. In these works, EBSD measurements are usually carried out on the undeformed sample so as to accurately reproduce grain geometries and orientations in the numerical model. The surface deformation of the oligocrystal under deformation is then recorded using digital image correlation or the grid method to obtain surface strain fields that can

be directly compared to their numerical counterparts. To the authors' best knowledge, this approach has not yet been applied to HCP metals, thus providing the motivation for the present work.

As a first approach, CRSS ratios identified in a previous study [1] for a grade 1 CP-Ti are used to examine the ability of a crystal plasticity model to predict the strain field distributions within a grade 2 CP-Ti tensile sample containing 32 grains. The first section briefly presents the experimental results obtained on the CP-Ti oligocrystal. The second section presents the associated numerical model, while the third section is dedicated to the comparison of experimental and numerical strain fields.

2. Experiment

The considered material is a grade 2 CP-Ti obtained from a plasma oven continuous casting elaboration process. A tensile test was performed on a flat dogbone sample with a thickness of 3 mm, containing 32 grains over its 20mm×12mm gauge section. Grain orientations and geometries were measured prior to the test by EBSD measurement. During the test, digital image correlation was used to record the surface strain evolution. The stress-strain curve and the axial strain field evolution during the test are summarized in figure 1.

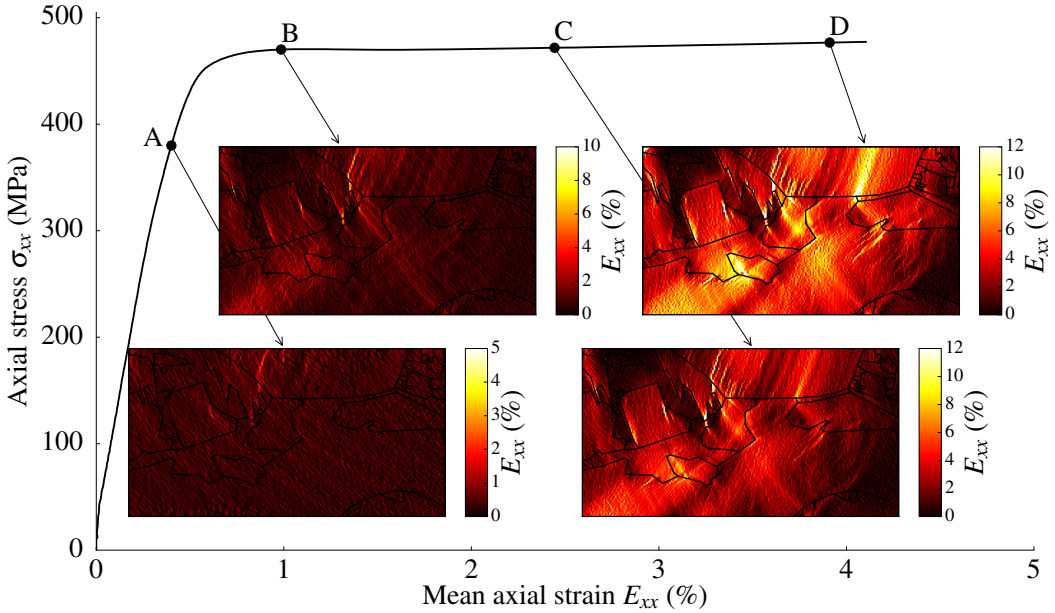

Figure 1. Axial strain evolution and stress strain curve for the tested sample

The recorded strain field distribution is highly heterogeneous throughout the test. Some grains experience up to 12 % axial strain locally, while others remain elastically deformed.

3. Numerical model

3.1. Crystal plasticity model

The model used in the authors' previous study [1] is applied to the description of the studied material. The slip rate evolution $\dot{\gamma}^{(\alpha)}$ for a slip system α is described by a visco-plastic power law [8] (eq.1):

$$\frac{\dot{\gamma}^{(\alpha)}}{\dot{\gamma}_0} = \left| \frac{\tau^{(\alpha)}}{\tau_Y^{(\alpha)}} \right|^{\frac{1}{m}} \text{sign}(\tau^{(\alpha)}) \quad , \quad \tau^{(\alpha)} = \boldsymbol{\sigma} : \left(\mathbf{s}^{(\alpha)} \otimes \mathbf{m}^{(\alpha)} \right) \tag{1}$$

where $\tau^{(\alpha)}$ is Schmid's resolved shear stress, and $\tau_Y^{(\alpha)}$ is the CRSS for slip system α. $\dot{\gamma}_0$ is the reference strain rate and m is the sensitivity exponent.

The evolution of CRSS is given by eq.2:

$$\dot{\tau}_Y^{(\alpha)} = \sum_\beta q_{\alpha\beta} h \left| \dot{\gamma}^{(\beta)} \right| \tag{2}$$

where $q_{\alpha\beta}$ is a component of the interaction matrix q, and h is the hardening rate. The summation in this equation is taken over both slip and twinning systems. Voce hardening is chosen for slip systems (eq. 3):

$$h(\bar{\gamma}) = h_0 \left(1 - \frac{\tau_0}{\tau_\infty} \right) \exp\left(-\frac{h_0 \bar{\gamma}}{\tau_\infty} \right) \tag{3}$$

where τ_0 is the initial CRSS, h_0 the initial hardening rate, and τ_∞ is the saturation value for τ. $\bar{\gamma}$ is the cumulative shear strain over all slip systems.

3.2. Mesh and boundary conditions

The mesh used for the simulations, based on the EBSD measurement of the undeformed sample, is presented in figure 2. Grain orientation is assumed constant within each grain, and columnar grain structure in the through thickness direction is assumed for all grains.

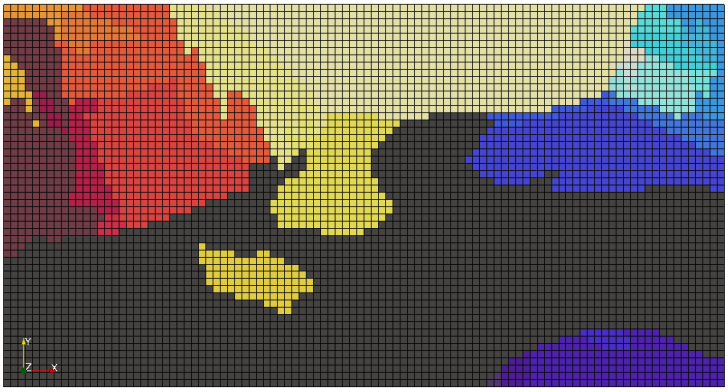

Figure 2. Mesh associated to grain geometries in the gauge section of the tested sample (extruded over 3 elements in the through thickness direction). Unique grain colors are assigned to mesh elements.

Displacement boundary conditions issued from the experimental DIC measurements are applied to the left and right faces of the model, while the upper and lower sections are free surfaces.

3.3. Material parameters

Since the studied sample contains a small number of grains, orthotropic elasticity is assumed in the simulation. The elastic moduli are given in table 1. Following previous modeling on a grade 1 CP-Ti [1], the rate sensitivity exponent and reference strain-rate are taken as m = 0.02 and $\dot{\gamma}_0$=0.001 s^{-1},

respectively. CRSS ratios are also conserved from this study, but higher CRSS values are used to account for the higher yield strength recorded on the present grade 2 CP-Ti material. These values are gathered in table 2. The reader is referred to reference [1] for the detail of the latent-hardening parameters.

C_{11}	C_{12}	C_{13}	C_{22}	C_{44}
157.9	93.4	69.4	177.4	45.3

Table 1. Anisotropic elastic moduli, expressed in GPa. $C_{33} = C_{22}$ and $C_{55} = C_{66} = C_{44}$.

	Basal	Prism.	Pyr.<a>	Pyr.<a+c>-1	Pyr.<a+c>-2	$\{10\bar{1}2\}$ twin.	$\{11\bar{2}2\}$ twin.
τ_0	332	155	202	363	363	225	350
τ_∞	450	400	521	673	673	/	/
h_0	1950	1050	580	2050	2050	350	350

Table 2. CRSS and hardening parameters used in the simulation, in MPa. CRSS values are adapted from reference [1]

4. Results and discussion

The axial strain field distribution at the end of the tensile test for the previous simulation is presented in figure 3, along with the corresponding experimental results.

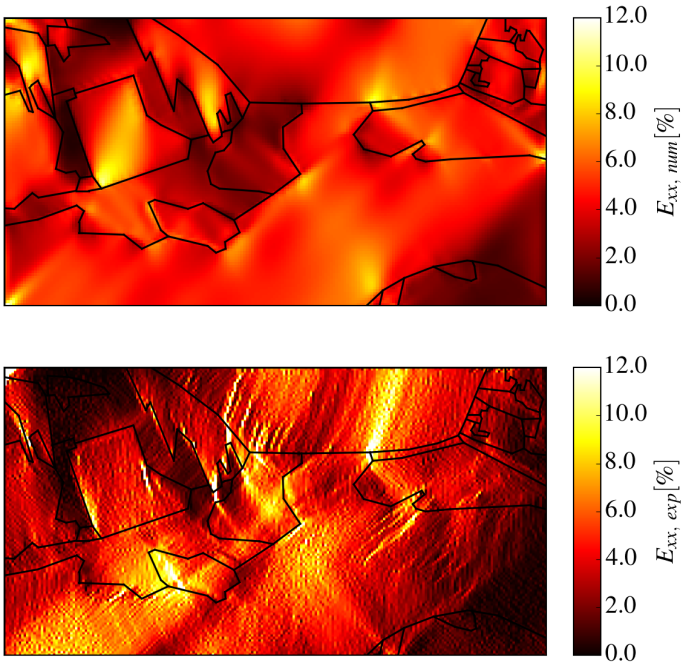

Figure 3. Axial strain field values at the end of tension test for the simulation (upper field) and experiment (lower field)

There is an overall good qualitative agreement between the experimental and numerical strain fields. Strain localizations within grains are reproduced in the simulations, and the least deformed areas also match the experimental ones. In particular, the simulation accurately reproduces strain localization arising near grain boundaries or triple points, suggesting that the modeling simplifications in grain shape and grain boundaries provide an acceptable approximation of the actual grain boundaries. Overall, local strain values are also in good agreement, suggesting that choosing grade 1 CP-TI CRSS ratios to reproduce the deformation behavior of the grade 2 CP-Ti sample is consistent.

5. Conclusion

Comparisons between the strain fields predicted by crystal plasticity analysis and their experimental counterparts have been carried out on a grade 2 CP-Ti oligocrystal. The heterogeneous strain distribution recorded experimentally is predicted satisfactorily for a model using the same CRSS ratios as identified on grade 1 CP-Ti. Future works will further this comparisons of experiment and simulations at the grain scale, to investigate the influence of different CRSS ratios on the model predictive capabilities. The activated slip systems within each grain will also be examined in detail numerically and experimentally.

Acknowledgements
This work has been funded by the Japan Society for the promotion of Science (JSPS) under the short term fellowship program (PE16708) and the authors gratefully acknowledge its support. TH also acknowledges the financial supports by JSPS KAKENHI Grant numbers 17H03428, and 17K06858.

References

[1] Hama T, Kobuki A, Takuda H. Crystal-plasticity finite-element analysis of anisotropic deformation behavior in a commercially pure titanium Grade 1 sheet. International Journal of Plasticity. 2017 Apr 1;91:77-108.
[2] Philippe MJ, Serghat M, Van Houtte P, Esling C. Modelling of texture evolution for materials of hexagonal symmetryII. application to zirconium and titanium or near alloys. Acta metallurgica et materialia. 1995 Apr 1;43(4):1619-30.
[3] Warwick JL, Jones NG, Rahman KM, Dye D. Lattice strain evolution during tensile and compressive loading of CP Ti. Acta Materialia. 2012 Nov 1;60(19):6720-31.
[4] Wang L, Zheng Z, Phukan H, Kenesei P, Park JS, Lind J, Suter RM, Bieler TR. Direct measurement of critical resolved shear stress of prismatic and basal slip in polycrystalline Ti using high energy X-ray diffraction microscopy. Acta Materialia. 2017 Jun 15;132:598-610.
[5] Zhao Z, Ramesh M, Raabe D, Cuitino AM, Radovitzky R. Investigation of three-dimensional aspects of grain-scale plastic surface deformation of an aluminum oligocrystal. International Journal of Plasticity. 2008 Dec 1;24(12):2278-97.
[6] Lim H, Carroll JD, Battaile CC, Buchheit TE, Boyce BL, Weinberger CR. Grain-scale experimental validation of crystal plasticity finite element simulations of tantalum oligocrystals. International Journal of Plasticity. 2014 Sep 1;60:1-8.
[7] Guery A, Hild F, Latourte F, Roux S. Slip activities in polycrystals determined by coupling DIC measurements with crystal plasticity calculations. International Journal of Plasticity. 2016 Jun 1;81:249-66.
[8] Peirce D, Asaro RJ, Needleman A. Material rate dependence and localized deformation in crystalline solids. Acta metallurgica. 1983 Dec 1;31(12):1951-76.